

pubs.acs.org/est Article

# Manganese Oxidation States in Volcanic Soils across Annual Rainfall Gradients

Ke Wen, Oliver A. Chadwick, Peter M. Vitousek, Elizabeth L. Paulus, Gautier Landrot, Ryan V. Tappero, John P. Kaszuba, George W. Luther, Zimeng Wang, Benjamin J. Reinhart, and Mengqiang Zhu\*



Cite This: Environ. Sci. Technol. 2023, 57, 730-740



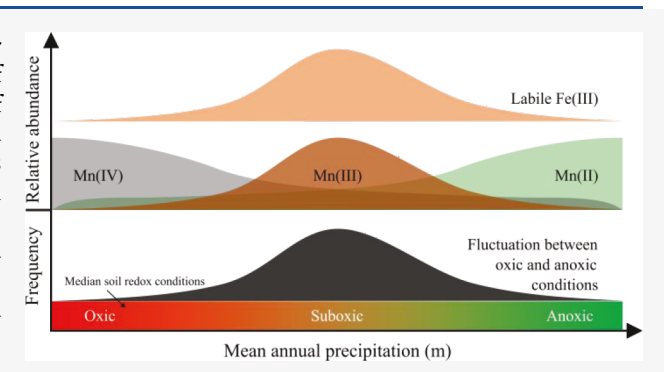
**ACCESS** I

Metrics & More

Article Recommendations

Supporting Information

ABSTRACT: Manganese (Mn) exists as Mn(II), Mn(III), or Mn(IV) in soils, and the Mn oxidation state controls the roles of Mn in numerous environmental processes. However, the variations of Mn oxidation states with climate remain unknown. We determined the Mn oxidation states in highly weathered bulk volcanic soils (primary minerals free) across two rainfall gradients covering mean annual precipitation (MAP) of 0.25–5 m in the Hawaiian Islands. With increasing MAP, the soil redox conditions generally shifted from oxic to suboxic and to anoxic despite fluctuating at each site; concurrently, the proportions of Mn(IV) and Mn(II) decreased and increased, respectively. Mn(III) was low at both low and high MAP, but accumulated substantially, up to 80% of total Mn, in soils with



prevalent suboxic conditions at intermediate MAP. Mn(III) was likely hosted in Mn(III,IV) and iron(III) oxides or complexed with organic matter, and its distribution among these hosts varied with soil redox potentials and soil pH. Soil redox conditions and rainfall-driven leaching jointly controlled exchangeable Mn(II) in soils, with its concentration peaking at intermediate MAP. The Mn redox chemistry was at disequilibrium, with the oxidation states correlating with long-term average soil redox potentials better than with soil pH. The soil redox conditions likely fluctuated between oxic and anoxic conditions more frequently at intermediate than at low and high MAP, creating biogeochemical hot spots where Mn, Fe, and other redox-sensitive elements may be actively cycled.

KEYWORDS: manganese oxidation states, soils, mean annual precipitation, redox fluctuations

#### ■ INTRODUCTION

Manganese (Mn) is a ubiquitous and highly redox-sensitive transition metal, <sup>1,2</sup> which exists in three oxidation states in natural environments, i.e., Mn(II), Mn(III), and Mn(IV). The Mn oxidation states and the electron transfer among them control the role of Mn in numerous environmental processes and elemental cycles. However, it remains unclear how climate affects the relative distribution of the three Mn oxidation states in soils, limiting our understanding of the environmental significance of Mn in global ecosystems.

The occurrence and biogeochemical behavior of Mn in environments highly depend on its oxidation state. Mn(II) is the common form in primary minerals and released to soils during weathering.<sup>4</sup> It is primarily soluble and required to support the biochemistry of photosynthesis for plants.<sup>5,6</sup> Mn(IV) exists as Mn(IV) oxides that are metal scavengers and strong oxidizers, influencing the fate of trace metals, organic compounds, and nutrients in the environment.<sup>7–9</sup> Solid Mn(III) exists as oxyhydroxides, oxides, or substitutes in other mineral structures;<sup>3</sup> dissolved Mn(III) tends to disproportionate to Mn(II) and Mn(IV) unless it binds to organic or inorganic ligands (L) to form stable or metastable Mn(III)—L complexes.<sup>10,11</sup> Mn(III)—L complexes are potent

oxidants and play key roles in depolymerizing lignin and other complex organic compounds during soil organic matter (SOM) and litter decomposition. <sup>12,13</sup> Mn cycles among the three oxidation states in response to the redox fluctuations. <sup>14</sup> Mn(II) can be oxidized by O<sub>2</sub> to Mn(III) or further to Mn(IV), <sup>15</sup> and conversely, Mn(IV) can be reduced to Mn(II) with Mn(III) as an intermediate product. <sup>16,17</sup> Abiotic processes are important in oxidation of Mn(II) under oxic conditions and reduction of Mn(III, IV) under reducing conditions as soils are rich in chemically reactive reductants, such as radicals in addition to O<sub>2</sub>. <sup>18–20</sup> However, the redox processes are often mediated by microorganisms, particularly for the formation of Mn(IV) oxides due to the slow kinetics of homogeneous abiotic oxidation of Mn(II) by O<sub>2</sub>. <sup>21,22</sup>

Received: April 14, 2022 Revised: November 30, 2022 Accepted: November 30, 2022 Published: December 20, 2022





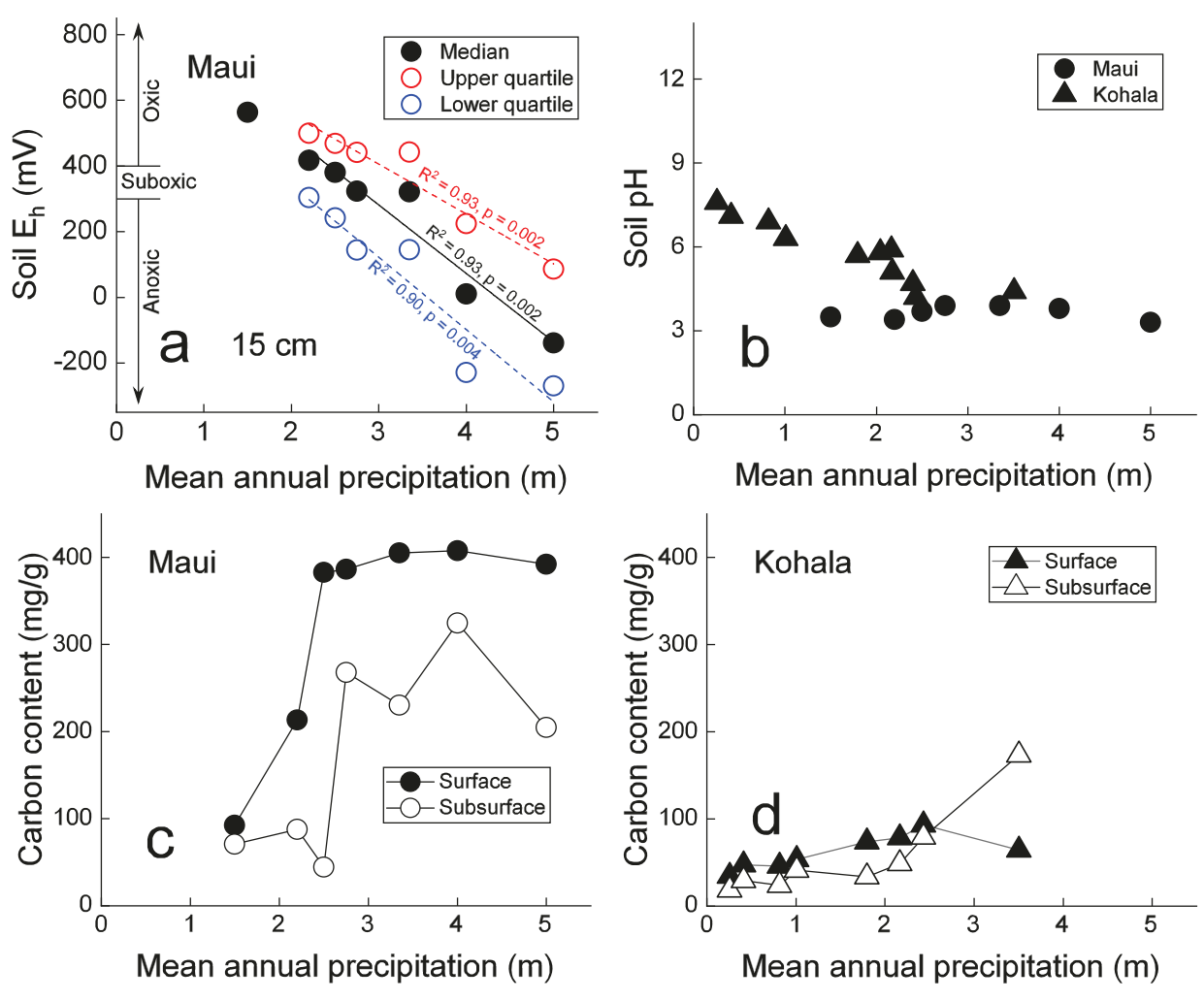


**Figure 1.** Soil redox potential  $(E_h)$ , pH, and carbon content of soils of the Maui and the Kohala rainfall gradients. The pH and  $E_h$  data of the Maui soils were reported previously, and adapted with permission from ref 29. Copyright 2001 John Wiley and Sons. The  $E_h$  values of the Maui soils were measured at monthly intervals over a year. The pH data of the Kohala soils were adapted with permission from ref 38. Copyright 2003 Elsevier. The  $E_h$  data of the Kohala soils are not available.

Climate is a master environmental variable that strongly influences soil water content, leaching, and vegetation, which in turn affect soil  $O_2$  availability, pH, mineralogy, and redox potentials. Annual rainfall positively and nonlinearly correlates with soil weathering. Rainfall can induce pedogenic thresholds and domains of soil physical, chemical, and biological processes, such as leaching loss of elements, soil pH, biological uplift, and redox conditions. Schuur et al. showed that soil  $E_{\rm h}$  varied systematically with mean annual precipitation (MAP) at Maui, Hawaii. With increasing MAP from 1.5 to 5 m, the median soil  $E_{\rm h}$  shifted from oxic ( $E_{\rm h} > 400$  mV) to suboxic ( $E_{\rm h} = 300-400$  mV) and to anoxic ( $E_{\rm h} < 300$  mV) despite fluctuations at each site (see more details below). Thus, MAP is expected to profoundly affect both the quantity and chemical forms of Mn in soils.

Thermodynamically,  $E_{\rm h}$  and pH jointly control the Mn oxidation states and the chemical forms in a system at equilibrium. According to the  $E_{\rm h}$ -pH diagram, as soil  $E_{\rm h}$  and/or pH increases, the dominant Mn oxidation state shifts from Mn(II) to Mn(III) and to Mn(IV). Accordingly, previous experimental measurements demonstrated that Mn(IV) predominates in oxic soils and Mn(II) in anoxic soils. Yet, it is unclear under what conditions Mn(III) is prevalent in

soils. Dissolved Mn(III)-ligand complexes were found to be abundant in suboxic aqueous environments, such as soil and sediment pore waters and water columns. 31-33 However, the predominance of Mn(III) in suboxic soil pore waters does not indicate its prevalence in bulk soils. In addition, soil is an open, multicomponent, and heterogeneous biogeochemical system that constantly exchanges materials and energy with the surroundings. Consequently, a soil system is usually far away from thermodynamic equilibrium,<sup>34</sup> and it is more challenging to predict the Mn oxidation states using the  $E_{\rm h}$ -pH diagram in soils than in the aqueous environment. Moreover, the  $E_{\rm h}$ -pH diagram, which is based on only a few solid and dissolved Mn species, may not be able to represent the actual Mn species in soils.<sup>35</sup> There are more than 30 different types of Mn (IV) oxides that differ in mineral structures and have unpredictable chemical compositions;<sup>3</sup> Mn(III) can also isomorphically substitute in minerals, such as iron (Fe) oxides.<sup>36</sup> While increased rainfall can lead to downward shifts in soil redox potentials and pH, 37,38 it is necessary to systematically determine the Mn oxidation states in soils to understand how rainfall influences the Mn redox geochemistry in soils.

In the present study, we determined the Mn oxidation states and the concentrations of total and exchangeable Mn in surface

and subsurface soil horizons from two broad and continuous gradients of rainfall in the Hawaiian Islands, while other soil development factors remained similar. We identified the rainfall regimes where Mn(III) was predominant and evaluated whether the Mn oxidation states of soils can be predicted using the  $E_{\rm h}$ –pH diagram. We also studied how soil redox conditions and rainfall-driven leaching jointly influence the concentrations of total and exchangeable Mn in soils. Furthermore, we discussed the frequency of soil redox fluctuations between oxic and anoxic conditions as a function of rainfall levels based on the accumulation of Mn(III) and labile Fe(III) oxides and evaluated why these accumulations peaked at intermediate rainfalls.

#### MATERIALS AND METHODS

Study Sites, Soil Sampling, and Pretreatment. The two rainfall gradients are separately located on the Islands of Maui (Haleakala Mountain) and Hawaii (Kohala Mountain), Hawaii (Figure S1). The Maui and Kohala rainfall gradients, respectively, consist of seven sites with MAP of 1.5-5.0 m<sup>2</sup> and 11 sites with MAP of 0.26-3.5 m<sup>38</sup> (Table S1). The mean annual temperature (MAT) remains at 16-17 °C at all Maui sites while it decreases from 23 to 17 °C with increasing MAP at the Kohala sites. The temporal variation in air temperature within a day or a year is up to 5 °C at these Kohala sites (http://climate.geography.hawaii.edu/).<sup>39</sup> Compared to the differences in rainfall (0.26-3.5 m) across the study sites, the temperature changes (from 23  $\pm$  5 to 17  $\pm$  5 °C) are much weaker and not expected to substantially affect Mn redox geochemistry in these soils. Except MAP and MAT, other soil formation factors remain nearly constant across the study sites of each gradient (Table S1). The parent materials are Kula lava at the Maui sites and Hawi lava at the Kohala sites, both containing ~1.7 mg/g of total Mn (Table S2). All Maui sites are covered by forests and all Kohala sites by grasslands except the wettest site which is covered mainly with forests. The soils had developed for 410 kiloyears (kyr) at the Maui sites and 150 kyr at the Kohala sites. All sites have low hillslopes ( $<5^{\circ}$ ). Kohala soils received severalfold higher dust inputs than Maui soils.40

The rainfall at each site varies little with season and it is only slightly higher in winter than in summer. Although the relatively low rainfall and high temperature in summer jointly result in drier soils than those in winter, the wettest Maui site is muddy most of the time in a year. Due to the relatively low solubility of O2 in water and its slow diffusion into soils, soil pores with a higher degree of water saturation are more reducing after the initial O<sub>2</sub> is depleted by microbial respiration. For a given soil, MAP largely controls the soil water saturation degree.  $^{41}$  The soil  $E_{\rm h}$  at each Maui site was in situ monitored monthly for a year using redox electrodes in the field with 10 replicates (Figure 1a) and reported previously.<sup>37</sup> The  $E_h$  fluctuates in the short term largely between suboxic ( $E_h$ = 300-400 mV) and oxic ( $E_h > 400$  mV) at the low rainfall sites, between anoxic ( $E_h$  < 300 mV) and oxic at the intermediate rainfall sites, and within the anoxic regime at the high rainfall sites (Figure 1a). The median, upper quartile (lowest values for upper 25% of measurements), and lower quartile (highest values for lowest 25% of measurements)  $E_h$ values over the long term across the gradient all decrease with increasing MAP. The median  $E_h$  shifts from oxic to anoxic with increasing MAP, with a suboxic regime occurring at intermediate rainfalls. These suggest strong controls of MAP

on soil  $E_h$  despite the fluctuations of  $E_h$  at each site. See more details about the  $E_h$  measurement of Maui soils in Text S1. The soil  $E_h$  was not measured for the Kohala gradient, but a similar relationship between  $E_h$  and MAP is expected because, like the Maui soils, the Kohala soils have similar particle size (clayey soils), organic matter, and biological features as the Maui soils.

Soil samples were collected from the top two mineral horizons (A and/or B) at the Maui sites in January 1997 and at the Kohala sites in April 1992. The first horizon was denoted as the surface soil and the second one as the subsurface soil. The subsurface soils were collected down to as deep as 23 cm at the Maui sites, and 92 cm at the Kohala sites (Table S1). All soils were dried and treated to remove plant debris after their collection. The Maui soils were oven-dried at 105 °C, and the Kohala soils were air-dried. The unground dry soils were subject to micro-X-ray fluorescence ( $\mu$ -XRF) and micro-Mn Kedge X-ray absorption near edge structure ( $\mu$ -XANES) spectroscopic analyses for distribution and speciation of Mn at the microscale. A portion of dried soil was ground and sieved to pass through a 100-mesh sieve prior to the soil extraction, chemical composition, and Mn K-edge XANES and X-ray diffraction (XRD) analyses for bulk Mn oxidation state and soil mineralogy. The same soil samples had been used in previous studies, and some basic soil chemical parameters were already reported. <sup>29,38</sup> With increasing MAP, soil pH remains at pH ~4 across the Maui gradient but decreases from 7.6 to 4.2 across the Kohala gradient (Figure 1b)29,38 because of the shorter development time and thus lower weathering degree of the Kohala soils.

Drying may concentrate  $H^+$  in soils and thus cause a reduction of Mn(III) and Mn(IV).<sup>42</sup> To determine the effects of drying on the Mn oxidation states, we collected additional soil samples at various soil depths from the pastureland near the sites of the Kohala gradient in June 2021. To maintain the soil moisture, the samples were packed into plastic zip bags of low-moisture transmission right after collection in the field and delivered with ice bags to a lab in Hawaii before storage at -80°C in a freezer. Then the frozen samples were shipped to Laramie, WY. Prior to characterization of the Mn oxidation states (see below), the soil samples were thawed at room temperature and gently homogenized. A subsample was frozen, and another one was oven-dried at 105 °C for the following bulk Mn K-edge XANES analysis. The differences in Mn oxidation states between the two subsamples indicate the effects of drying, by assuming that the Mn in frozen soils is not altered in terms of its oxidation state by interacting with X-rays during the XANES data collection, like that in dried soils.<sup>43</sup>

Characterization of Soil Samples. The XRD data of soils were collected at the beamline 17-BM-B ( $\lambda$  = 0.451 92 Å), Advanced Photon Source (APS), Argonne National Laboratory. Details for the XRD data collection and analysis are provided in Text S2.

The total Mn concentrations of soil samples were measured using inductively coupled plasma optical emission spectrometry (ICP-OES, PerkinElmer Optima 8300) after a digestion of Li-metaborate fusion beads with aqua regia. The exchangeable Mn was extracted from each soil sample by shaking  $\sim$ 0.2 g of soils with 10 mL of MgCl<sub>2</sub> solution (1 mol/L) at pH 7 for 1 h, after which the suspension was filtered using 0.45  $\mu$ m membrane filters. The Mn concentration in filtrates was measured using the ICP-OES. The labile Fe oxides in soils were extracted by acid ammonium oxalate in the dark, while the crystalline Fe oxides (the residue of the oxalate extraction)

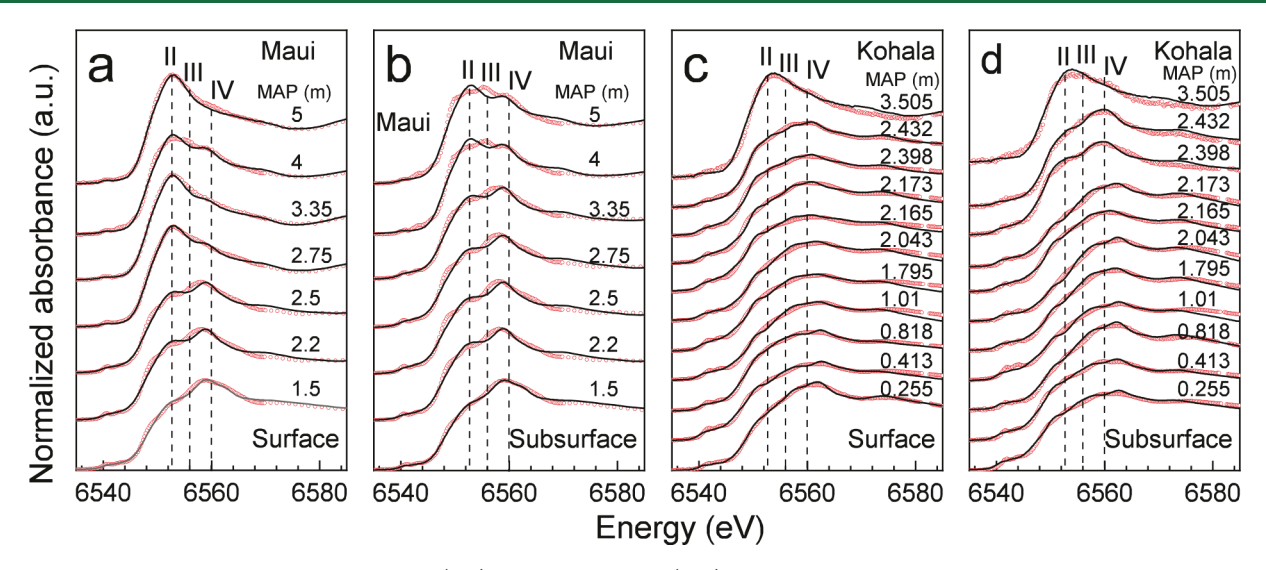


Figure 2. Mn K-edge XANES spectra of the surface (a, c) and the subsurface (b, d) soils of the Maui and the Kohala rainfall gradients. The number besides each spectrum is the mean annual precipitation (MAP, m) of the study site.

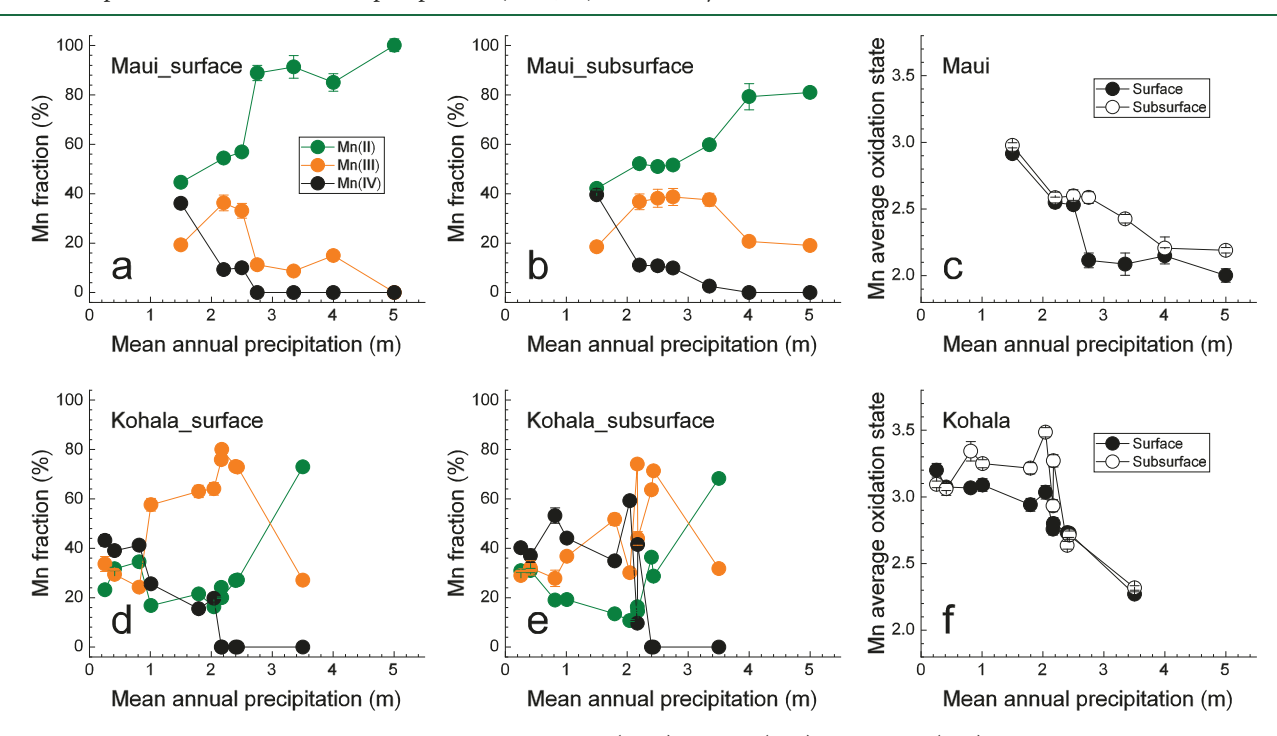


Figure 3. Fractions of different Mn oxidation states and their average (AOS) in Maui (a-c) and Kohala (d-f) soils. The Mn oxidation states were obtained from the LCF analyses of the Mn XANES spectra. The error bars represent the fitting errors derived from the LCF analysis.

were extracted by citrate-dithionate bicarbonate.<sup>38</sup> The total organic carbon in soils was measured using an elemental analyzer (Carlo Erba CN2100).

The Mn oxidation states in soils were determined using a combination of XANES spectroscopy and a linear combination fitting (LCF) analysis.  $^{13,30}$  The spectra were collected at beamline 7-3 or beamline 4-1 at Stanford Synchrotron Radiation Lightsource, SLAC National Accelerator Laboratory, United States, or SAMBA beamline at synchrotron SOLEIL, France. A preliminary test for some samples was conducted at beamline 12-BM-B, Advanced Photon Source, Argonne National Laboratory. The  $\mu$ -XRF and  $\mu$ -XANES analyses were conducted at the XFM beamline (4-BM), National Synchrotron Light Source-II. All dried soil powders were measured at ambient conditions except for those used for

checking effects of drying, which were measured on a cryostage along with their corresponding frozen samples. A Mn metal foil reference was concomitantly measured with each sample for internal energy calibration ( $E_0 = 6539 \text{ eV}$ ).

A pool of Mn reference XANES spectra (Table S3) was employed for the LCF analyses. MnSO<sub>4</sub>(aq), MnO, and Mn(II) complexed with humic acid were used as Mn(II) references while Ca<sub>2</sub>Mn<sub>3</sub>O<sub>8</sub>, a layered Mn oxide, was used as a Mn(IV) reference. Mn(III) references include hausmannite [33% of Mn(II) and 67% of Mn(III)], manganite, a Mn(III)—pyrophosphate solution, and Mn-substituted hematite[14% of Mn(II), 72% of Mn(III), and 14% of Mn(IV)]. Reference materials other than those listed above were tested but were found not to contribute to the fittings. Energy shifts were not

allowed during the LCF analyses. More details about the Mn XANES characterization are provided in Text S3.

The average oxidation state (AOS) of Mn in each soil sample was calculated according to eq 1 with its uncertainty estimated using eq 2:

$$AOS = 4 \times f_{IV} + 3 \times f_{III} + 2 \times f_{II}$$
 (1)

AAOS

$$= \sqrt{(4 \times f_{\text{IV}})^2 (\Delta f_{\text{IV}})^2 + (3 \times f_{\text{III}})^2 (\Delta f_{\text{III}})^2 + (2 \times f_{\text{II}})^2 (\Delta f_{\text{III}})^2}$$
(2)

where  $f_{\rm IV}, f_{\rm III}$ , and  $f_{\rm II}$  represent the atomic fraction of Mn(IV), Mn(III), and Mn(II), determined from the XANES LCF analyses;  $\Delta f_{\rm IIV}$ ,  $\Delta f_{\rm III}$ , and  $\Delta f_{\rm II}$  are the corresponding fitting uncertainties of the LCF results.

#### ■ RESULTS AND DISCUSSION

**Soil Mineralogy.** Due to the high weathering, neither the soils of the Maui nor those of the Kohala gradients contain detectable primary minerals according to the XRD analysis (Figure S2). Thus, primary minerals, in which Mn exists as Mn(II) and Mn(III),<sup>47</sup> did not contribute to the Mn pool of our soils, and all Mn were hosted in secondary minerals. Halloysite, quartz, hematite, and maghemite are the major minerals in the soils. However, due to the low concentrations in soils, no Mn oxides, oxyhydroxides, or carbonates, if present, were detected by XRD. The following XANES analysis provides more information on Mn-bearing mineral phases.

**Mn Oxidation States.** The Mn oxidation states of soils vary greatly and systematically with MAP for both the Maui and the Kohala gradients. With increasing MAP, the XANES spectral features of Mn(IV) gradually attenuate while those of Mn(II) become increasingly pronounced for the Maui surface soils (Figure 2a). As MAP increases from 2.5 to 2.75 m, the dominant spectral feature abruptly switches from Mn(IV) to Mn(II). The spectral features suggest that the subsurface soil (Figure 2b) contains more oxidized and less reduced Mn than does the corresponding surface soil (Figure 2a). The XANES LCF analysis determines the relative atomic fraction of each Mn oxidation state in soils, and the results are consistent with the above qualitative analyses based on the spectral features. In the Maui surface soils, as MAP increases, the Mn(IV) fraction monotonically decreases from 36% to 0%, while the Mn(II) fraction increases from 45% to 100% (Figure 3a and Table S4). Consistent with the spectral features, the Mn(II) fraction increases abruptly from 57% to 89% as MAP increases from 2.5 to 2.75 m. Notably, the fitting identifies an accumulation of Mn(III) (33-36%) in soils at intermediate rainfalls (2.2-2.5 m) with lower Mn(III) proportions at both low and high rainfalls. The subsurface soils demonstrate similar but more gradual patterns of variation of Mn oxidation states with MAP (Figure 3b). The MAP regime, where Mn(III) is prevalent, is wider in the subsurface soils than in the surface soils. The Mn AOS in soils decreases with increasing MAP, and the subsurface soil has a higher Mn AOS than the surface soil (Figure 3c). Although Mn(IV) is not identified in the Maui soils at 4.0 m of MAP by the bulk XANES due to the low sensitivity of the analysis, it is detected at the microscale by  $\mu$ -XANES analysis (Figure S3f, spot 15 and 19). The  $\mu$ -XANES results also suggest substantial microscale heterogeneity in Mn oxidation states in soils (Figure S3).

The soil  $E_{\rm h}$ , rather than soil pH, appears to be the primary variable that determines the Mn oxidation states because soil pH at the Maui gradient does not vary with rainfall levels (pH ~4, Figure 1b). With increasing MAP from 1.5 to 5 m, the median redox condition of the Maui soils gradually shifts from oxic to suboxic (slightly oxidizing and slightly reducing) and eventually reaches anoxic conditions (Figure 1a). Also, the subsurface soils were more oxidizing than the surface soils (Figure S4), consistent with a recent study. 48 Although the soils are presumably not at thermodynamic equilibrium, the changes of Mn oxidation states with mean soil Eh follow the general pattern that Mn(IV) and Mn(II) prevail in oxidizing and reducing conditions, respectively. The abrupt increase of the Mn(II) fraction is likely caused by the switch of median  $E_h$ from suboxic ( $E_h$  = 400–300 mV) to anoxic ( $E_h$  < 300 mV), where the occurrence of neither Mn(III) nor Mn(IV) is favorable. Consistently, Hindersmann and Mansfeldt<sup>49</sup> found a sharp increase of exchangeable Mn(II) in soils when redox conditions shifted from suboxic to reducing ( $E_h$  < 300 mV). The substantial accumulation of Mn(III) in suboxic soils at intermediate rainfalls was observed in the field for the first time, although the accumulation of dissolved Mn(III) at oxic/ anoxic interfaces was discovered previously in laboratory soil column incubation experiments, 13 as well as other suboxic natural waters. 31,32 The Mn(III) accumulation in the Maui subsurface soils covers a wider range of MAP (2.2-3.35 m) than it does in the surface soils probably due to the more oxidizing soil conditions in the subsurface (Figure S4). The more oxidizing subsurface is also consistent with the higher Mn AOS in the subsurface soils. Overall, our results suggest that the Mn redox chemistry in bulk soils is likely related to the long-term average rather than short-term fluctuating soil redox conditions. The short-term fluctuating redox conditions may be more relevant to the dynamics of exchangeable Mn(II) and/or labile Mn(III,IV) pools, which warrants future investigations.

The XANES spectra of the Kohala soils are quite different from those of the Maui soils at similar MAP (Figure 2c,d), suggesting a different composition of Mn oxidation states. However, a similar pattern of the Mn oxidation state versus MAP, particularly at MAP > 1.5 m, also occurs for the Kohala gradient, though less regular than that of the Maui gradient (Figure 3d,e). Notably, the Mn(III) fractions of the Kohala surface soils are much higher than those of the Maui surface soils at a given MAP, with the maximum reaching 80% at 2.5 m of MAP (Figure 3a,d, and Table S5). The Mn AOS is also higher for the Kohala soils than the Maui soils at a given MAP (Figure 3c,f). The high Mn(III) fraction in the Kohala surface soils, compared to those of the Maui surface soils, is likely caused by the higher soil pH (Figure 1b) and the lower SOM content in these pasture soils compared with the forest soils of Maui (Figure 1c,d). Elevated pH favors the occurrence of Mn(III,IV) rather than Mn(II) according to the  $E_h$ -pH diagram, while a high SOM content favors the occurrence of Mn(II) because SOM can reduce Mn(III) and Mn(IV). 18

As reported by Ross et al.,  $^{42}$  we find drying may cause a reduction of Mn(IV) to Mn(II), although the influence likely depends on soil pH (Figure S5). When the soil pH is higher than 4.7, drying has slight or no effects on the Mn oxidation states for most of the soils. However, substantial overestimation of Mn(II) (10–27%) and underestimation of Mn(IV) (10–33%) occurred in soils with pH < 4.7 (Figure S5b). Thus, the overestimation of Mn(II) and the under-

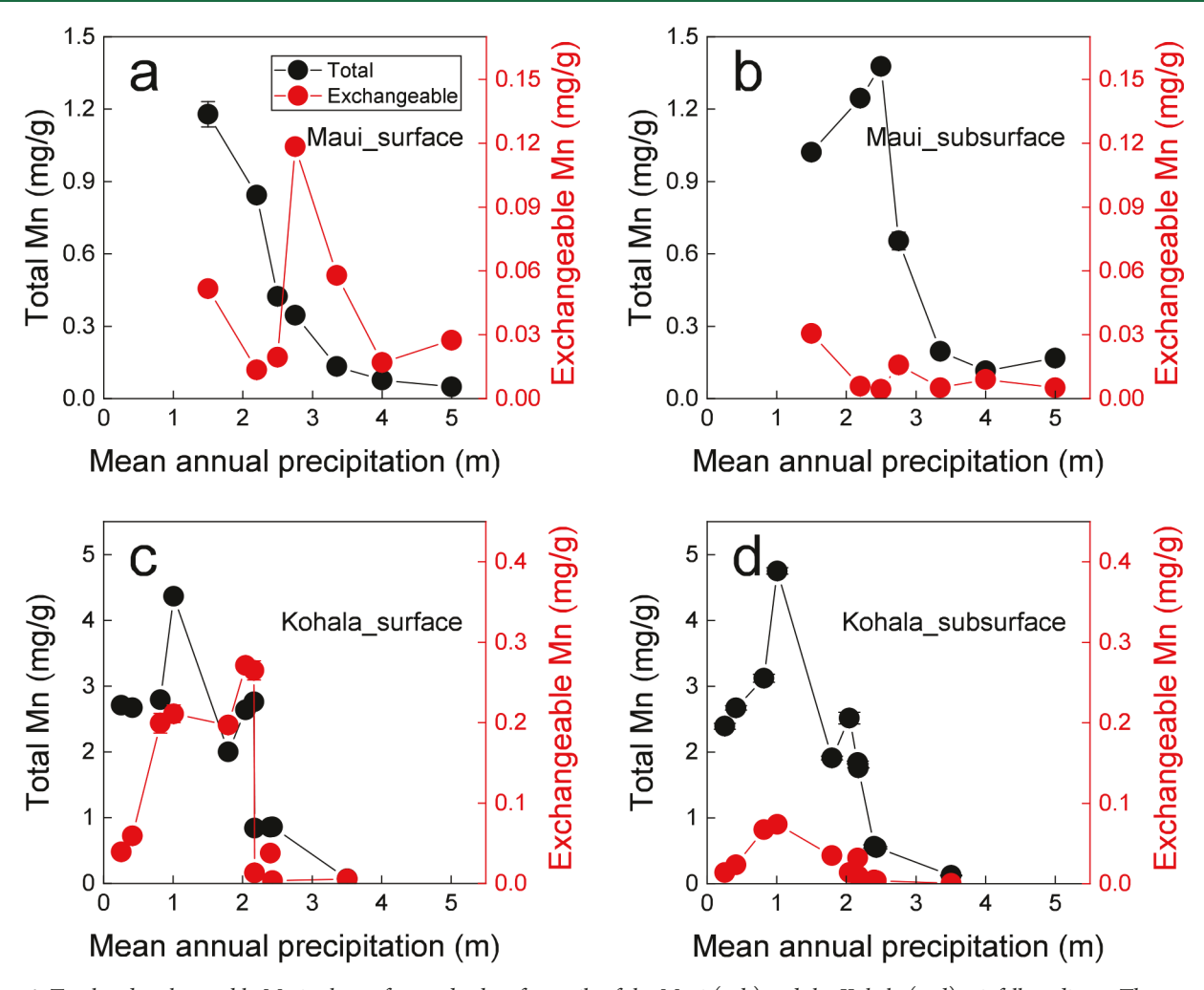


Figure 4. Total and exchangeable Mn in the surface and subsurface soils of the Maui (a, b) and the Kohala (c, d) rainfall gradients. The error bars represent the standard deviation derived from two repeated experiments.

estimation of Mn(IV) likely occur to the same degree across the Maui gradient, while they only occur at the Kohala site with MAP > 3.1 m. However, the observed patterns of Mn(II) and Mn(IV) are likely to hold because highly reducing conditions at high MAP favor the presence of Mn(II) but not Mn(IV). Different from Mn(II) and Mn(IV), drying only slightly affects the Mn(III) fraction and causes an overestimation of only 6% at most regardless of soil pH (Figure S5b), too small to be responsible for the remarkably different Mn(III) fractions observed across each gradient.

Mn-Bearing Phases. Despite the uncertainties associated with the XANES LCF analysis in identifying Mn chemical forms, XANES LCF can provide insights into the possible phases of the Mn-bearing solids. The requirement of a layered structure, Ca<sub>2</sub>Mn<sub>3</sub>O<sub>8</sub>, to represent Mn(IV) species for the fitting (Tables S4 and S5) suggests the possible presence of layer Mn(IV) oxides in soils. The Mn(III) species may include hausmannite (Mn<sub>3</sub>O<sub>4</sub>), Mn-substituted hematite, manganite (γ-MnOOH), and dissolved Mn(III)—pyrophosphate complexes. The potential occurrence of Mn-substituted hematite in the acidic Maui soils suggests that Mn(III) substitutes for Fe(III) in Fe(III) oxides, consistent with the strong Fe—Mn spatial correlations at the microscale (Figure S3). Since Fe(III) oxides are more thermodynamically stable than Mn oxides under acidic conditions, the substitution can stabilize Mn(III) in the acidic Maui soils, although the

Mn(III)-substituted Fe(III) oxides may be less stable than the pure Fe(III) oxides due to the structural distortion. 46,53 Mn(III)-pyrophosphate can occur in soils but may also represent Mn(III)-organic complexes that can be stable in acidic environments, 13 such as acidic forest soils 54 and during acidic treatment of marine Mn(III)-humic complexes.3 Thermodynamically, neither discrete Mn(III) nor Mn(IV) oxides form under the relatively strong acidic conditions of the Maui soils and the wetter Kohala soils. The occurrence of Mn(III) and Mn(IV) oxides can be attributed to the presence of less acidic soil microsites, such as the microenvironments around microbial cells. 55-57 Their occurrence may also be caused by slow or even no responses to reducing conditions if they are physically occluded by less redox active mineral particles in microaggregates. The MnSO<sub>4</sub> solution and humic acid-complexed Mn(II) can jointly represent soluble Mn(II) and Mn(II) bound to the common exchange phases, i.e., SOM and phyllosilicates, in soils. MnCO<sub>3</sub> may also contribute to the Mn(II) pool in the weakly alkaline soils at the driest Kohala sites, although including MnCO3 as a reference did not improve the linear combination fitting of the XANES spectra.

Total and Exchangeable Mn. Rainfall greatly changes the concentrations of both total and bioavailable Mn in soils. With increasing MAP, the total Mn concentration in Maui soils decreased monotonically whereas the concentration of exchangeable Mn(II), an index of available Mn, increased

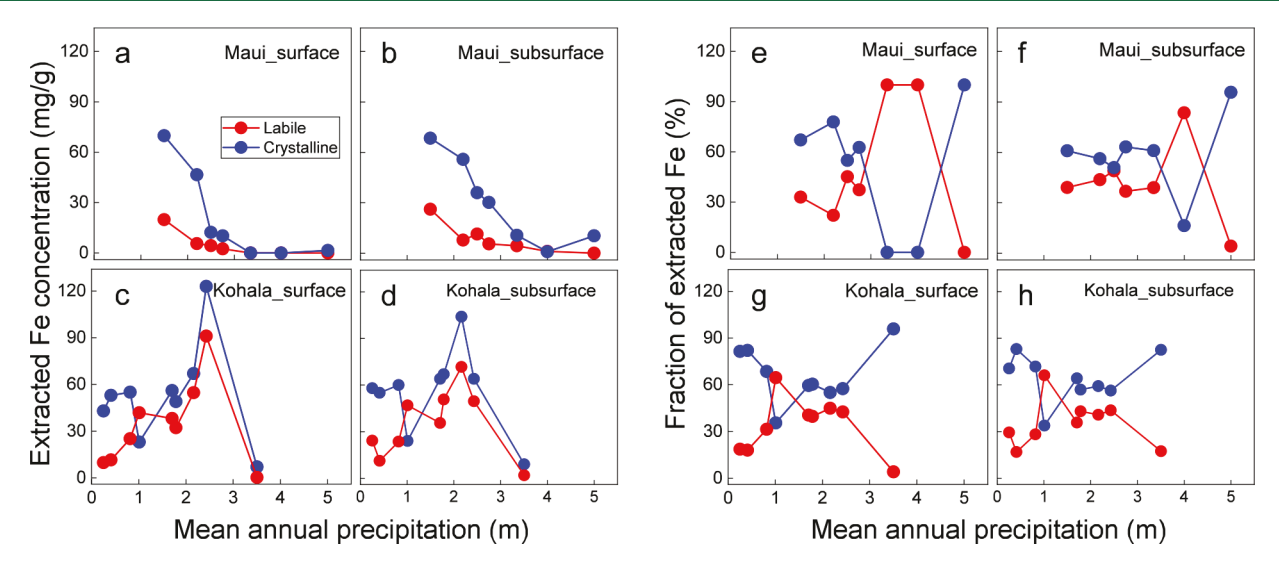


Figure 5. Concentrations (a-d) and fractions (e-h) of extractable labile and crystalline Fe in surface and subsurface soils of the Maui and the Kohala rainfall gradients.

and then decreased (Figure 4a). The decrease in total Mn is caused by increasingly intensive rainfall-driven leaching loss of Mn. The exchangeable Mn(II) reaches a maximum at intermediate rainfalls, coinciding with the abrupt increase of total Mn(II) in soils (Figure 3a) due to the shift of soil redox conditions from suboxic to more reducing conditions (Figure 1a). These observations are consistent with a previous report that dissolved Mn(II) concentration sharply increased when soil  $E_{\rm h}$  was lowered to moderately reducing conditions.<sup>49</sup> The abrupt changes of exchangeable Mn(II) concentrations with MAP in Maui (and the Kohala) soils also align with the pedogenic thresholds associated with the initiation of anoxic conditions and the mobilization of Fe(III) oxides at about 2.5 m of MAP. 58,59 However, the remarkably high leaching intensity and the strongly reducing soil conditions at high rainfalls jointly and effectively remove Mn from soils, thus leading to the declines of both the total and exchangeable Mn(II) as MAP continues to increase (Figure 4a). The total Mn concentration in the Maui subsurface soils increased with MAP up to MAP = 2.5 m, followed by a decline. The increase suggests that the subsurface soils gained more Mn from downward leaching out of the surface soils than the loss of Mn, and that the difference increased until MAP beyond 2.5 m where the loss overwhelmed due to the high rainfall and the more reducing conditions. Compared to the surface soils, the concentration of exchangeable Mn(II) in the subsurface soils is much lower (Figure 4b). The high exchangeable Mn(II) in surface soils can be attributed to the more reducing conditions, a higher SOC content, and plant uplift of soluble Mn from subsurface soils. 13,59

Compared to the Maui soils, the concentrations of total Mn and exchangeable Mn(II) are much higher in both surface and subsurface Kohala soils (Figure 4), attributed to the younger soil age and higher pH, hence less leaching loss, as well as the higher dust accretion at the Kohala sites. The total Mn concentration increased with MAP up to MAP = 1 m, which could be caused by increasing preferential depletion of mobile alkali and alkaline earth metal cations (e.g., Na<sup>+</sup>, K<sup>+</sup>, and Ca<sup>2+</sup>) relative to Mn<sup>2+</sup>, as indicated by the index ( $\tau$ ) of elemental gain and loss (Figure S6). Mn is not vulnerable to leaching loss as much as those redox-inert cations due to the immobilization

of  $\rm Mn^{2+}$  by oxidative precipitation as  $\rm Mn(III,IV)$  oxides in these oxic soils. The total Mn concentration in the Kohala soils began to decrease at MAP > 2.2 m, suggesting the dominance of leaching-driven loss of Mn, as for Maui soils. With increasing MAP, the exchangeable Mn(II) concentration increased and reached maxima at MAP = 0.8–2.4 m and decreased thereafter. Like for the Maui gradient, the pattern of exchangeable Mn(II) could be attributed to the joint control of leaching and  $E_{\rm h}$ , as well as the declining soil pH. The variations of the exchangeable Mn(II) with MAP are also partially caused by the accumulation and depletion of total Mn, particularly for the Kohala subsurface soils for which the concentrations of the two Mn pools positively correlate (Figure 4d). This is not surprising as reductive dissolution of Mn(III,IV) is a source of exchangeable Mn(II).

Note that the reduction of Mn(IV) during sample drying may increase exchangeable Mn(II) in the Maui and Kohala soils at high MAP, but it should not contribute much to the accumulation of Mn(II) in the Kohala soils at the low and intermediate rainfalls where the extent of Mn(IV) reduction due to drying was low.

Redox Fluctuations and Mn(III) Accumulation. The observed patterns of the Mn oxidation states may also be contributed by the relative frequency of soil redox fluctuations between oxic and anoxic conditions under different MAP. While the accumulation of solid Mn(III) at intermediate rainfalls is thermodynamically consistent with the prevalent suboxic soil conditions there, we argue that the accumulation may also be kinetically controlled as a result of soil redox fluctuations due to soil hydrological processes. A recent conceptual model states that redox fluctuations result in the formation of redox-active metastable phases (RAMPs), whose properties cannot be predicted a priori from standard free energies.<sup>60</sup> RAMPs exist because the residence time of one redox state (e.g., oxic) of the system is relatively short before switching to another state (e.g., anoxic), not allowing RAMPs to have enough time to ripen toward products of higher stability, unless the ripening process is disturbed by external forces. 60 Thus, frequent redox fluctuations would result in abundant RAMPs relative to those ripened phases, and the

relative abundance of RAMPs may serve as an indicator of the frequency of redox fluctuations in a system.

Mn(III) species are likely RAMPs as they can both accept and donate electrons. 16 Our observed accumulation of Mn(III) in soils at the intermediate rainfall would suggest that soil redox conditions fluctuate across the oxic and anoxic boundary so frequently that there is not enough time for the majority of Mn(III) to be reduced to Mn(II) when under anoxic conditions or oxidized to Mn(IV) when under oxic conditions. Such a pattern of redox fluctuation was indeed observed at the intermediate rainfall sites of Maui (Figure 1a). The results also imply that the majority of the Mn(III) species in soils must not be as reactive as free Mn(III) species; 2 otherwise, it would respond rapidly to soil  $E_h$  changes, which is not the case. The relatively low reactivity of Mn(III) could be caused by the occlusion of Mn(III) oxides and oxyhydroxides within microsites that are not readily accessible by reducing substances, or Mn(III) substitution in other mineral structures (e.g., Fe oxides). Despite soil  $E_h$  fluctuating widely, the fluctuation occurred mainly within the oxic regime at the low rainfall and within the anoxic regime at the high rainfall. Consequently, the majority of the Mn(III) species is oxidized or reduced, resulting in the dominance of Mn(IV) and Mn(II), respectively.

The above dependence of the frequency of soil redox fluctuation between oxic and anoxic conditions on rainfall levels is further suggested by labile Fe(III) oxides, which are RAMPs and include ferrihydrite, 60 across the rainfall gradients. Consistent with the high frequency of soil redox fluctuations between oxic and anoxic conditions at the intermediate rainfalls, labile Fe(III) accumulated proportionally at the intermediate rainfalls, relative to the low and high rainfalls for both Maui and Kohala gradient regardless of the surface or subsurface soils (Figure 5). The accumulation of labile Fe(III) phases was also indicated in the data reported by Thompson et al., who examined different soils from those in the present study but also across the Maui rainfall gradient. 61,62 Under the frequent redox fluctuation between oxic and anoxic conditions, the Fe redox cycle is quite active, and labile Fe(III) species have limited time to crystallize before being reduced and entering the next redox cycle. In contrast, labile Fe(III) phases, once formed, are readily transformed to well-crystallized ones under dominantly oxic conditions at low rainfall, and reductively dissolved or crystallized by Fe(II) catalysis under dominantly reducing conditions at high rainfall.61-64 Soil organic matter can complex and stabilize labile Fe, 65-67 which, however, is unlikely to be the primary reason for the observed pattern across the rainfall gradient. This is because the SOC concentrations were high at the high rainfalls, but the proportions of labile Fe were low.

The dependence of the soil redox fluctuation frequency between oxic and anoxic conditions on rainfall levels can be understood from the perspective of soil  $O_2$  and  $H_2O$  contents. The overall oxic conditions in soils at the low rainfall are poised by high  $O_2$  and low  $H_2O$  content in soil pores (away from water saturation), and soil  $E_h$  does not often fluctuate much into anoxic conditions. At high rainfalls, the soil pores are often saturated, and the reducing conditions are poised by the high  $H_2O$  and low  $O_2$  contents<sup>59</sup> so that soil  $E_h$  rarely enters the oxic regime. However, suboxic conditions are likely not poised well at the intermediate rainfalls because neither  $O_2$  nor  $H_2O$  content is overwhelming, and soil pores can

frequently shift between oxic and anoxic conditions, as we observed (Figure 1a).

#### **■ ENVIRONMENTAL IMPLICATIONS**

Compared to Mn(II) and Mn(IV), conditions favoring the occurrence of Mn(III) in terrestrial ecosystems remain unclear. Here, we showed that prevalent suboxic soil conditions and likely a high frequency of redox fluctuation between oxic and anoxic conditions created by intermediate rainfalls favored the accumulation of solid Mn(III) in highly weathered, primary mineral free clayey volcanic soils. Our findings suggest that Mn(III) can accumulate in the clay size fraction of other types of soils under certain rainfall levels that induce suboxic conditions. Soil aggregates often have a redox gradient at the structural microscale, 68,69 across which Mn may shift from Mn(II) to Mn(III) and to Mn(IV) spatially from the core to the outer shell of the aggregate. Our findings, however, may not be applied to bulk sandy soils that have a low water retention capacity, a large proportion of macropores, and thus are often oxidizing. The identified dependence of Mn(III) on redox conditions may apply to environmental settings other than soils. For example, solid Mn(III) may dominate the Mn speciation in suboxic zones of ocean water columns and sediments.<sup>31–33</sup> While not measured, soluble Mn(III)-L complexes are likely significant and have a relatively long lifetime in settings where solid Mn(III) species are prevalent, as both occur favorably under suboxic conditions. Since it is challenging to accurately detect and quantify soluble Mn(III)— L complexes in soils, 54,70 solid Mn(III) in soils could serve as an indicator for the activity of Mn(III)-mediated degradation of natural organic matter. Besides, the Mn(III) center in the mixed-valence Mn(III,IV) oxides may be more reactive than the Mn(IV) counterparts in oxidation of reducing compounds. 71,72 The likely high frequency of redox fluctuations between oxic and anoxic conditions in soils at the intermediate rainfalls suggests that the soils are biogeochemical hot spots where Mn, Fe, and likely other redox-active elements can be actively cycled. 60 Overall, the role of Mn in the environmental and ecological processes varies with MAP, and future studies are warranted to examine if the observed MAP dependence holds regardless of the type of the soils, such as coarse-textured soils, nonvolcanic soils, alkaline soils, and soils containing primary minerals, in diverse ecosystems at larger geospatial scales. Future investigations are also needed to determine responses of soil Mn pools of different reactivity to redox fluctuations of varying frequency.

#### ASSOCIATED CONTENT

#### **Solution** Supporting Information

The Supporting Information is available free of charge at https://pubs.acs.org/doi/10.1021/acs.est.2c02658.

Descriptions of the soil pH and  $E_{\rm h}$ , collection of Mn K-edge XANES spectra, soil extractions, collection and analyses of synchrotron X-ray diffraction (XRD) data, XRD patterns, maps of study sites, microscale distribution of Mn and Fe and  $\mu$ -XANES of Mn, monthly variations of soil  $E_{\rm h}$  (50 cm depth) across the Maui rainfall gradient, soil properties, chemical compositions of parent materials and soil samples at the Maui and the Kohala sites, and the Mn reference pool used for LCF fitting and the corresponding fitting results (PDF)

#### AUTHOR INFORMATION

#### **Corresponding Author**

Mengqiang Zhu — Department of Ecosystem Science and Management, University of Wyoming, Laramie, Wyoming 82071, United States; Orcid.org/0000-0003-1739-1055; Email: mzhu6@uwyo.edu

#### **Authors**

- Ke Wen Department of Ecosystem Science and Management, University of Wyoming, Laramie, Wyoming 82071, United States; © orcid.org/0000-0002-2080-6541
- Oliver A. Chadwick Department of Geography, University of California, Santa Barbara, California 93106, United States
- Peter M. Vitousek Department of Biology, Stanford University, Stanford, California 94305, United States
- Elizabeth L. Paulus Department of Biology, Stanford University, Stanford, California 94305, United States
- Gautier Landrot Synchrotron SOLEIL, L'Orme des Merisiers, Saint Aubin 91190, France; orcid.org/0000-0001-7673-421X
- Ryan V. Tappero Brookhaven National Laboratory, NSLS-II, Upton, New York 11973, United States
- John P. Kaszuba Department of Geology and Geophysics and School of Energy Resources, University of Wyoming, Laramie, Wyoming 82071, United States; ⊙ orcid.org/0000-0001-8799-0673
- George W. Luther School of Marine Science and Policy, University of Delaware, Lewes, Delaware 19958, United States
- Zimeng Wang Department of Environmental Science and Engineering, Fudan University, Shanghai 200438, China; orcid.org/0000-0002-4572-629X
- Benjamin J. Reinhart Argonne National Laboratory, Chicago, Illinois 60439, United States; orcid.org/0000-0001-5654-8823

Complete contact information is available at: https://pubs.acs.org/10.1021/acs.est.2c02658

#### **Notes**

The authors declare no competing financial interest.

#### ACKNOWLEDGMENTS

This work was supported by United States National Science Foundation under DEB-2027284. This research utilized resources of the Stanford Synchrotron Radiation Lightsource beamline 4-1 and 7-3 operated for the U.S. Department of Energy (DOE) Office of Science by the Stanford Linear Accelerator Center National Accelerator Laboratory under Contact No. DE-AC02-76SF00515, the Advanced Photon Source beamline 12-BM and mail-in program at beamline 17-BM-B operated for the DOE Office of Science by Argonne National Laboratory under Contract No. DE-AC02-06CH11357, and the National Synchrotron Light Source-II XFM beamline operated for the DOE Office of Science by Brookhaven National Laboratory under Contract No. DE-SC0012704. Synchrotron SOLEIL was also acknowledged for provision of synchrotron radiation facilities.

#### ■ REFERENCES

(1) Namgung, S.; Chon, C.-M.; Lee, G. Formation of diverse Mn oxides: A review of bio/geochemical processes of Mn oxidation. *Geosci. J.* **2018**, *22*, 373–381.

- (2) Tebo, B. M.; Bargar, J. R.; Clement, B. G.; Dick, G. J.; Murray, K. J.; Parker, D.; Verity, R.; Webb, S. M. Biogenic manganese oxides: properties and mechanisms of formation. *Annu. Rev. Earth Planet. Sci.* **2004**, *32* (1), 287–328.
- (3) Post, J. E. Manganese oxide minerals: Crystal structures and economic and environmental significance. *Proc. Natl. Acad. Sci. U. S. A.* 1999, 96 (7), 3447–3454.
- (4) Crerar, D. A.; Cormick, R. K.; Barnes, H. L.Geochemistry of Manganese: An overview. In *Geology and Geochemistry of Manganese*; Varentsov, I. M., Grasselly, G., Eds.; Schweizerbartsche Verlagsbuchhandlung: Stuttgart, Germany, 1980; Vol. 1, pp 293–334.
- (5) Cheniae, G.; Martin, I. Photoreaction of manganese catalyst in photosynthetic oxygen evolution. *Plant Physiol.* **1969**, 44 (3), 351–360
- (6) Morgan, J. J.Manganese in natural waters and earth's crust: Its availability to organisms. In *Met. Ions Biol. Syst.*; Sigel, A., Sigel, H., Eds.; CRC Press, 2000; Vol. 37, pp 1–34.
- (7) Villalobos, M.; Bargar, J.; Sposito, G. Trace metal retention on biogenic manganese oxide nanoparticles. *Elements* **2005**, *1* (4), 223–226
- (8) Yao, W.; Millero, F. J. Adsorption of phosphate on manganese dioxide in seawater. *Environ. Sci. Technol.* **1996**, *30*, 536–541.
- (9) Li, H.; Santos, F.; Butler, K.; Herndon, E. A critical review on the multiple roles of manganese in stabilizing and destabilizing soil organic matter. *Environ. Sci. Technol.* **2021**, *55* (18), 12136–12152.
- (10) Qian, A.; Zhang, W.; Shi, C.; Pan, C.; Giammar, D. E.; Yuan, S.; Zhang, H.; Wang, Z. Geochemical stability of dissolved Mn(III) in the presence of pyrophosphate as a model ligand: Complexation and disproportionation. *Environ. Sci. Technol.* **2019**, *53* (10), 5768–5777.
- (11) Duckworth, O. W.; Sposito, G. Siderophore-manganese(III) interactions. I. Air-oxidation of manganese(II) promoted by desferrioxamine B. *Environ. Sci. Technol.* **2005**, *39* (16), 6037–6044.
- (12) Keiluweit, M.; Nico, P.; Harmon, M. E.; Mao, J.; Pett-Ridge, J.; Kleber, M. Long-term litter decomposition controlled by manganese redox cycling. *Proc. Natl. Acad. Sci. U. S. A.* **2015**, *112* (38), E5253–E5260.
- (13) Jones, M. E.; Nico, P. S.; Ying, S.; Regier, T.; Thieme, J.; Keiluweit, M. Manganese-driven carbon oxidation at oxic—anoxic interfaces. *Environ. Sci. Technol.* **2018**, *52* (21), 12349–12357.
- (14) Morgan, J. J. Chemistry of aqueous manganese II and IV: A thesis; Harvard University, 1964.
- (15) Morgan, J. J. Kinetics of reaction between  $O_2$  and Mn(II) species in aqueous solutions. *Geochim. Cosmochim. Acta* **2005**, 69 (1), 35–48
- (16) Luther, G. W. Manganese(II) oxidation and Mn(IV) reduction in the environment—Two one-electron transfer steps versus a single two-electron step. *Geomicrobiol. J.* **2005**, 22 (3–4), 195–203.
- (17) Canfield, D. E.; Thamdrup, B.; Hansen, J. W. The anaerobic degradation of organic matter in Danish coastal sediments: Iron reduction, manganese reduction, and sulfate reduction. *Geochim. Cosmochim. Acta* **1993**, 57 (16), 3867–3883.
- (18) Ma, D.; Wu, J.; Yang, P.; Zhu, M. Coupled manganese redox cycling and organic carbon degradation on mineral surfaces. *Environ. Sci. Technol.* **2020**, *54* (14), 8801–8810.
- (19) Jung, H.; Xu, X.; Wan, B.; Wang, Q.; Borkiewicz, O. J.; Li, Y.; Chen, H.; Lu, A.; Tang, Y. Photocatalytic oxidation of dissolved Mn(II) on natural iron oxide minerals. *Geochim. Cosmochim. Acta* **2021**, 312, 343–356.
- (20) Jung, H.; Snyder, C.; Xu, W.; Wen, K.; Zhu, M.; Li, Y.; Lu, A.; Tang, Y. Photocatalytic oxidation of dissolved Mn<sup>2+</sup> by TiO<sub>2</sub> and the formation of tunnel structured manganese oxides. *ACS Earth Space Chem.* **2021**, *5* (8), 2105–2114.
- (21) Tebo, B. M.; Johnson, H. A.; McCarthy, J. K.; Templeton, A. S. Geomicrobiology of manganese(II) oxidation. *Trends Microbiol.* **2005**, 13 (9), 421–428.
- (22) Learman, D. R.; Voelker, B. M.; Vazquez-Rodriguez, A. I.; Hansel, C. M. Formation of manganese oxides by bacterially generated superoxide. *Nat. Geosci.* **2011**, *4*, 95.

- (23) Slessarev, E. W.; Lin, Y.; Bingham, N. L.; Johnson, J. E.; Dai, Y.; Schimel, J. P.; Chadwick, O. A. Water balance creates a threshold in soil pH at the global scale. *Nature* **2016**, *540* (7634), 567–569.
- (24) Brady, N. C.; Weil, R. R.; Weil, R. R.Formation of soils from parent materials. In *The nature and properties of soils*; Prentice Hall: Upper Saddle River, NJ, 2008; Vol. 13, pp 32–75.
- (25) Sugihara, S.; Shibata, M.; Mvondo Ze, A. D.; Araki, S.; Funakawa, S. Effect of vegetation on soil C, N, P and other minerals in Oxisols at the forest-savanna transition zone of central Africa. *Soil Sci. Plant Nutr.* **2014**, *60* (1), 45–59.
- (26) Chadwick, O. A.; Chorover, J. The chemistry of pedogenic thresholds. *Geoderma* **2001**, *100* (3), 321–353.
- (27) Teutsch, N.; Erel, Y.; Halicz, L.; Chadwick, O. A. The influence of rainfall on metal concentration and behavior in the soil. *Geochim. Cosmochim. Acta* **1999**, *63* (21), 3499–3511.
- (28) Porder, S.; Hilley, G. E.; Chadwick, O. A. Chemical weathering, mass loss, and dust inputs across a climate by time matrix in the Hawaiian Islands. *Earth Planet. Sci. Lett.* **2007**, 258 (3), 414–427.
- (29) Schuur, E. A. G.; Chadwick, O. A.; Matson, P. A. Carbon cycling and soil carbon storage in mesic to wet Hawaiian montane forests. *Ecology* **2001**, 82 (11), 3182–3196.
- (30) Guest, C. A.; Schulze, D. G.; Thompson, I. A.; Huber, D. M. Correlating manganese X-ray absorption near-edge structure spectra with extractable soil manganese. *Soil Sci. Soc. Am. J.* **2002**, *66* (4), 1172–1181.
- (31) Trouwborst, R. E.; Clement, B. G.; Tebo, B. M.; Glazer, B. T.; Luther, G. W. Soluble Mn(III) in suboxic zones. *Science* **2006**, *313* (5795), 1955–1957.
- (32) Madison, A. S.; Tebo, B. M.; Mucci, A.; Sundby, B.; Luther, G. W. Abundant porewater Mn (III) is a major component of the sedimentary redox system. *Science* **2013**, 341 (6148), 875–878.
- (33) Oldham, V. E.; Mucci, A.; Tebo, B. M.; Luther, G. W. Soluble Mn (III)-L complexes are abundant in oxygenated waters and stabilized by humic ligands. *Geochim. Cosmochim. Acta* **2017**, *199*, 238-246.
- (34) Kleidon, A. A basic introduction to the thermodynamics of the Earth system far from equilibrium and maximum entropy production. *Philos. Trans. R. Soc. B-Biol. Sci.* **2010**, 365 (1545), 1303–1315.
- (35) Birkner, N.; Navrotsky, A. Thermodynamics of manganese oxides: Sodium, potassium, and calcium birnessite and cryptomelane. *Proc. Natl. Acad. Sci. U. S. A.* **2017**, *114* (7), E1046–E1053.
- (36) Manceau, A.; Schlegel, M. L.; Musso, M.; Sole, V. A.; Gauthier, C.; Petit, P. E.; Trolard, F. Crystal chemistry of trace elements in natural and synthetic goethite. *Geochim. Cosmochim. Acta* **2000**, *64* (21), 3643–3661.
- (37) Schuur, E. A.; Matson, P. A. Net primary productivity and nutrient cycling across a mesic to wet precipitation gradient in Hawaiian montane forest. *Oecologia* **2001**, *128* (3), 431–442.
- (38) Chadwick, O. A.; Gavenda, R. T.; Kelly, E. F.; Ziegler, K.; Olson, C. G.; Elliott, W. C.; Hendricks, D. M. The impact of climate on the biogeochemical functioning of volcanic soils. *Chem. Geol.* **2003**, 202 (3), 195–223.
- (39) Giambelluca, T.; Shuai, X.; Barnes, M.; Alliss, R.; Longman, R.; Miura, T.; Chen, Q.; Frazier, A.; Mudd, R.; Cuo, L. Evapotranspiration of Hawai'i; Report for US Army Corps of Engineers—Honolulu District, and the Commission on Water Resource Management, State of Hawai'i, 2014.
- (40) Kurtz, A. C.; Derry, L. A.; Chadwick, O. A. Accretion of Asian dust to Hawaiian soils: isotopic, elemental, and mineral mass balances. *Geochim. Cosmochim. Acta* **2001**, *65* (12), 1971–1983.
- (41) O'Connell, C. S.; Ruan, L.; Silver, W. L. Drought drives rapid shifts in tropical rainforest soil biogeochemistry and greenhouse gas emissions. *Nat. Commun.* **2018**, 9 (1), 1348.
- (42) Ross, D. S.; Hales, H. C.; Shea-McCarthy, G. C.; Lanzirotti, A. Sensitivity of soil manganese oxides: Drying and storage cause reduction. *Soil Sci. Soc. Am. J.* **2001**, *65* (3), 736–743.
- (43) Ross, D. S.; Hales, H. C.; Shea-McCarthy, G. C.; Lanzirotti, A. Sensitivity of soil manganese oxides: XANES spectroscopy may cause reduction. *Soil Sci. Soc. Am. J.* **2001**, *65* (3), 744–752.

- (44) Hossner, L.Dissolution for total elemental analysis. In *Methods* of *Soil Analysis Part 3: Chemical Methods*; Sparks, D. L., Page, A. L., Helmke, P. A., Loeppert, R. H., Eds.; John Wiley & Sons, 1996; pp 49–64.
- (45) Zimmerman, A. J.; Weindorf, D. C. Heavy metal and trace metal analysis in soil by sequential extraction: A review of procedures. *Int. J. Anal. Chem.* **2010**, *2010*, 1.
- (46) Li, W.; Wang, Q.; Feng, X.; Tan, W.; Zheng, L.; Yin, H.; Liu, F. The distinct effects of isomorphous substitution of various divalence trace metals on hematite structure. *Mater. Chem. Phys.* **2018**, 217, 40–47.
- (47) Zhang, Z.; Liu, C.; Zhao, Z.; Cui, L.; Liu, W.; Liu, T.; Liu, B.; Fan, B. Behavior of redox-sensitive elements during weathering of granite in subtropical area using X-ray absorption fine structure spectroscopy. *J. Asian Earth Sci.* **2015**, *105*, 418–429.
- (48) Aeppli, M.; Thompson, A.; Dewey, C.; Fendorf, S. Redox properties of solid phase electron acceptors affect anaerobic microbial respiration under oxygen-limited conditions in floodplain soils. *Environ. Sci. Technol.* **2022**, *56*, 17462–17470.
- (49) Hindersmann, I.; Mansfeldt, T. Trace element solubility in a multimetal-contaminated soil as affected by redox conditions. *Water Air Soil Pollut.* **2014**, 225 (10), 2158.
- (50) Mc Kenzie, R. M.Manganese oxides and hydroxides. In *Minerals in Soil Environments*; Soil Science Society of America: Madison, WI, 1989; pp 439–465.
- (51) Saratovsky, I.; Wightman, P. G.; Pastén, P. A.; Gaillard, J.-F.; Poeppelmeier, K. R. Manganese oxides: Parallels between abiotic and biotic structures. *J. Am. Chem. Soc.* **2006**, *128* (34), 11188–11198.
- (52) Dublet, G.; Juillot, F.; Brest, J.; Noël, V.; Fritsch, E.; Proux, O.; Olivi, L.; Ploquin, F.; Morin, G. Vertical changes of the Co and Mn speciation along a lateritic regolith developed on peridotites (New Caledonia). *Geochim. Cosmochim. Acta* **2017**, 217, 1–15.
- (53) Li, W.; Wang, L.; Liu, F.; Liang, X.; Feng, X.; Tan, W.; Zheng, L.; Yin, H. Effects of Al<sup>3+</sup> doping on the structure and properties of goethite and its adsorption behavior towards phosphate. *J. Environ. Sci.* **2016**, *45*, 18–27.
- (54) Jones, M. E.; LaCroix, R. E.; Zeigler, J.; Ying, S. C.; Nico, P. S.; Keiluweit, M. Enzymes, manganese, or iron? Drivers of oxidative organic matter decomposition in soils. *Environ. Sci. Technol.* **2020**, *54* (21), 14114–14123.
- (55) Richardson, L. L.; Aguilar, C.; Nealson, K. H. Manganese oxidation in pH and O<sub>2</sub> microenvironments produced by phytoplankton. *Limnol. Oceanogr.* **1988**, 33 (3), 352–363.
- (56) Sparrow, L. A.; Uren, N. C. Oxidation and reduction of Mn in acidic soils: Effect of temperature and soil pH. *Soil Biol. Biochem.* 1987, 19 (2), 143–148.
- (57) Mayanna, S.; Peacock, C. L.; Schäffner, F.; Grawunder, A.; Merten, D.; Kothe, E.; Büchel, G. Biogenic precipitation of manganese oxides and enrichment of heavy metals at acidic soil pH. *Chem. Geol.* **2015**, 402, 6–17.
- (58) Miller, A. J.; Schuur, E. A. G.; Chadwick, O. A. Redox control of phosphorus pools in Hawaiian montane forest soils. *Geoderma* **2001**, *102* (3), 219–237.
- (59) Vitousek, P. M.; Chadwick, O. A. Pedogenic thresholds and soil process domains in basalt-derived soils. *Ecosystems* **2013**, *16* (8), 1379–1395.
- (60) Peiffer, S.; Kappler, A.; Haderlein, S. B.; Schmidt, C.; Byrne, J. M.; Kleindienst, S.; Vogt, C.; Richnow, H. H.; Obst, M.; Angenent, L. T.; Bryce, C.; McCammon, C.; Planer-Friedrich, B. A biogeochemical—hydrological framework for the role of redox-active compounds in aquatic systems. *Nat. Geosci.* 2021, 14 (5), 264–272.
- (61) Thompson, A.; Rancourt, D. G.; Chadwick, O. A.; Chorover, J. Iron solid-phase differentiation along a redox gradient in basaltic soils. *Geochim. Cosmochim. Acta* **2011**, 75 (1), 119–133.
- (62) Thompson, A.; Ruiz, J.; Chadwick, O. A.; Titus, M.; Chorover, J. Rayleigh fractionation of iron isotopes during pedogenesis along a climate sequence of Hawaiian basalt. *Chem. Geol.* **200**7, 238 (1), 72–83.

- (63) Thompson, A.; Chadwick, O. A.; Rancourt, D. G.; Chorover, J. Iron-oxide crystallinity increases during soil redox oscillations. *Geochim. Cosmochim. Acta* **2006**, *70* (7), 1710–1727.
- (64) Thompson, A.; Chadwick, O. A.; Boman, S.; Chorover, J. Colloid mobilization during soil iron redox oscillations. *Environ. Sci. Technol.* **2006**, *40* (18), 5743–5749.
- (65) Karlsson, T.; Persson, P.; Skyllberg, U.; Mörth, C.-M.; Giesler, R. Characterization of iron(III) in organic soils using extended X-ray absorption fine structure spectroscopy. *Environ. Sci. Technol.* **2008**, 42 (15), 5449–5454.
- (66) Schwertmann, U. Inhibitory effect of soil organic matter on the crystallization of amorphous ferric hydroxide. *Nature* **1966**, 212 (5062), 645–646.
- (67) Eusterhues, K.; Wagner, F. E.; Häusler, W.; Hanzlik, M.; Knicker, H.; Totsche, K. U.; Kögel-Knabner, I.; Schwertmann, U. Characterization of ferrihydrite-soil organic matter coprecipitates by X-ray diffraction and mössbauer spectroscopy. *Environ. Sci. Technol.* 2008, 42 (21), 7891–7897.
- (68) Keiluweit, M.; Wanzek, T.; Kleber, M.; Nico, P.; Fendorf, S. Anaerobic microsites have an unaccounted role in soil carbon stabilization. *Nat. Commun.* **2017**, 8 (1), 1771.
- (69) Keiluweit, M.; Gee, K.; Denney, A.; Fendorf, S. Anoxic microsites in upland soils dominantly controlled by clay content. *Soil Biol. Biochem.* **2018**, *118*, 42–50.
- (70) Keiluweit, M.; Bougoure, J. J.; Nico, P. S.; Pett-Ridge, J.; Weber, P. K.; Kleber, M. Mineral protection of soil carbon counteracted by root exudates. *Nat. Clim. Chang.* **2015**, *5* (6), 588.
- (71) Wang, Q.; Yang, P.; Zhu, M. Effects of metal cations on coupled birnessite structural transformation and natural organic matter adsorption and oxidation. *Geochim. Cosmochim. Acta* **2019**, 250, 292–310.
- (72) Wang, Q.; Yang, P.; Zhu, M. Structural transformation of birnessite by fulvic acid under anoxic conditions. *Environ. Sci. Technol.* **2018**, 52 (4), 1844–1853.

### ☐ Recommended by ACS

### Seasonal Oxygenation of Contaminated Floodplain Soil Releases Zn to Porewater

Christian Dewey, John R. Bargar, *et al.*MARCH 14, 2023
ENVIRONMENTAL SCIENCE & TECHNOLOGY

READ 🗹

#### Manganese in Groundwater in South Asia Needs Attention

M. Feisal Rahman, Peter Ravenscroft, et al.

OCTOBER 05, 2022

ACS ES&T WATER

READ

## Effects of C/Mn Ratios on the Sorption and Oxidative Degradation of Small Organic Molecules on Mn-Oxides

Hui Li, Elizabeth Herndon, et al.

DECEMBER 19, 2022

ENVIRONMENTAL SCIENCE & TECHNOLOGY

READ 🗹

#### Historic and Contemporary Surface Disposal of Produced Water Likely Inputs Arsenic and Selenium to Surficial Aquifers

Robert J. Rossi, Dominic C. DiGiulio, et al.

MAY 05, 2023

ENVIRONMENTAL SCIENCE & TECHNOLOGY

READ **C** 

Get More Suggestions >